

## LEARNING LOCAL DIRECTED ACYCLIC GRAPHS BASED ON MULTIVARIATE TIME SERIES DATA \*

BY WANLU DENG AND ZHI GENG AND HONGZHE LI

*Peking University and University of Pennsylvania*

Multivariate time series (MTS) data such as time course gene expression data in genomics are often collected to study the dynamic nature of the systems. These data provide important information about the causal dependency among a set of random variables. In this paper, we introduce a computationally efficient algorithm to learn directed acyclic graphs (DAGs) based on MTS data, focusing on learning the local structure of a given target variable. Our algorithm is based on learning all parents (P), all children (C) and some descendants (D) (PCD) iteratively, utilizing the time order of the variables to orient the edges. This time series PCD-PCD algorithm (tsPCD-PCD) extends the previous PCD-PCD algorithm to dependent observations and utilizes composite likelihood ratio tests (CLRTs) for testing the conditional independence. We present the asymptotic distribution of the CLRT statistic and show that the tsPCD-PCD is guaranteed to recover the true DAG structure when the faithfulness condition holds and the tests correctly reject the null hypotheses. Simulation studies show that the CLRTs are valid and perform well even when the sample sizes are small. In addition, the tsPCD-PCD algorithm outperforms the PCD-PCD algorithm in recovering the local graph structures. We illustrate the algorithm by analyzing a time course gene expression data related to mouse T-cell activation.

**1. Introduction.** Inferring causal networks among a set of genes based on their expression levels is one of the most important problems in genomics. High-throughput technologies such as microarrays or next generation sequencing have enabled biologists to measure expression levels of all the genes in large-scale. Technologies are also available to obtain gene expressions at single-cell level for inference of single-cell expression dynamics. Time-course gene expression experiments where the expression levels of the genes measured over time during a biological process are particularly important in providing dynamic information about gene regulation and networks (Buganim et al., 2012). The focus of this paper is on learning the local graphs based on such multivariate time course gene expression data.

---

\*Research supported by NIH grants R01CA127334 and R01GM097505.

*Keywords and phrases:* Bayesian network, Composite likelihood ratio test, Genetic network, PCD-PCD algorithm

Graphical models have been applied to study gene networks based on gene expression data, among which Gaussian graphical models are most commonly used and studied (Schäfer and Strimmer, 2005; Li and Gui, 2006; Li et al., 2013). However, the Gaussian graphical models only provide information on conditional independence and the resulting graphs are undirected. Alternatively, directed acyclic graphs (DAGs) are frequently used to represent independence, conditional independence and causal relationships among random variables in a complex system (Pearl, 2000; Spirtes, Glymour and Scheines, 2000). In such DAG models, parents of some nodes in the graph are understood as “causes,” and edges have the meaning of “causal influences.” The causal influences among random variables imply conditional independence relations among them. Murphy and Mian (1999) and Friedman et al. (2000) have suggested using Bayesian network models of gene expression networks.

Methods for learning the structures of DAGs include the search-and-score based methods (Cooper and Herskovits, 1992; Heckerman, 1995; Chickering, 2002; Friedman and Koller, 2003) that require elicitation of all the conditional probabilities and the constraint-based methods (Neapolitan, 2003) that evaluate the presence or absence of an edge by testing conditional independence among variables. These constraint-based learning methods often require unreasonable amounts of data in order to accurately estimate higher order conditional independence relations from finite samples. Algorithms that combine ideas from constraint-based and search-and-score techniques have also been developed and have shown excellent performance (Tsamardinos, Brown and Aliferis, 2006). Efficient Markov chain Monte Carlo methods have also been developed for learning the Bayesian networks (Friedman and Koller, 2003; Ellis and Wong, 2008).

Most of the current available methods for structural learning of DAGs assume that the data are *i.i.d* samples from some joint distribution specified by the underlying DAG. These methods cannot be directly applied to multivariate time series (MTS) data. One approach to causal graph learning from the MTS data is based on the dynamic Bayesian network (DBN) model (Ghahramani, 1997), which is an extension of the Bayesian network model for time series data. DBN models the stochastic evolution of a set of random variables over time. In comparison with Bayesian network, discrete time is introduced and conditional distributions are related to the values of parent variables in the previous time point. Moreover, in DBNs the acyclicity constraint is relaxed. Husmeier (2003) studied the sensitivity and specificity of inferring genetic regulatory interactions from microarray experiments with DBNs. Grzegorzcyk and Husmeier (2011) presented methods for improve-

ments in the reconstruction of time-varying gene regulatory networks using dynamic programming and regularization by information sharing among genes. Rau et al. (2010) proposed to apply the linear Gaussian state-space models, a subclass of DBNs, for estimating biological network from time course gene expression data with replications.

The DAG structural learning algorithms (Pearl, 2000; Spirtes, Glymour and Scheines, 2000; Heckerman, 1995; Tsamardinos, Brown and Aliferis, 2006) have mainly focused on constructing the whole directed graph over all the variables. Such whole directed graphs are often difficult to learn due to small sample sizes or limited perturbation to the underlying system to infer the causal relationships. In some applications, one might be interested in identifying the causal variables of a given node and the variables that this node influences, i.e., in identifying the local structure of a variable. In genomics, we might be interested in learning the upstream regulators of a gene and also the downstream genes regulated by this gene. Methods for learning the local directed graphs have many practical applications and play a central role in causal discovery and classification because of their scalability benefits. One key concept in learning local causal graph structure is the Markov blanket of a variable  $T$ , which is a minimal variable subset conditioning on which all other variables are probabilistically independent of  $T$ . Finding the Markov blanket has been the basis of many of the newly developed methods for learning DAG structures (Margaritis and Thrun, 2000; Tsamardinos, Aliferis and Statnikov, 2003; Tsamardinos, Brown and Aliferis, 2006).

Yin et al. (2008) developed a partial orientation and local structure learning algorithm based on identifying all parents (P), all children (C) and some descendent (D) of a given node. This algorithm is called PCD-PCD algorithm. Zhou et al. (2010) further extended this algorithm by constructing a larger local network with depth  $d$  and using a more efficient stopping rule to reduce the computation time. Like many other structural learning algorithms, PCD-PCD is based on the tests of conditional independence among a set of variables. Yin et al. (2008); Zhou et al. (2010) used the standard likelihood ratio tests (LRTs) for conditional independence testing. However, such tests cannot be applied directly to MTS data due to the dependency of the data observed over time.

In this paper, we propose to extend PCD-PCD to MTS data in order to learn a local network around a target variable. We consider stationary ergodic MTS with time-invariant dependence structure. In our approach, search for separators of a pair of variables in a large DAG is localized to small subsets, and thus the approach can improve the efficiency of searches and the

power of statistical tests for structural learning. Our approach captures the Bayesian dynamic nature of the dependence by learning the structure of the graphical model based on conditional independence between the past and future of observations of the time series. The new method utilizes the time order to orient edges connecting variables at different time points. Like the PCD-PCD algorithm, we first find parents, children and some descendants of the target  $T$  to obtain a local skeleton with a radius 1, and then repeatedly find PCDs of the nodes in the previous PCDs until the radius of the local skeleton is up to the given depth  $d$ . By focusing on learning the local DAGs, the proposed algorithm can handle high dimensional random variables even when the sample size is not too large.

Since the conditional independence test plays a key role in our proposed algorithm, we develop composite likelihood ratio tests (CLRTs) for conditional independence for MTS data taking into account the dependency of the variables over time. The commonly used likelihood ratio test for conditional independence is invalid under the small sample size when the null hypothesis only involves variables at the same time point. The CLRT statistic enables us to perform valid inference on conditional independency under the setting of small sample sizes, allowing the number of independent time series smaller than the number of variables at each time point.

In Section 2, we present the local structural learning algorithm tsPCD-PCD for multivariate time series data. In Section 3, we develop the CLRTs for conditional independence for time series data. We then present simulation results to evaluate the algorithm and the validity of the CLRTs in Section 4 and application of the method to analysis of gene expression data related to T-cell activation in Section 5. Finally, we give a brief discussion of the methods in Section 6. The exact statements of the theorems and their proofs can be found in Online Supplemental Material.

## 2. Algorithm for Learning a Local Structure Around a Target Variable.

*2.1. Statistical model, data observed and notation.* We consider the data from MTS where the lag of the time series is  $q$  and there are  $p$  variables at each time point. Let  $\mathbf{X}_t = (X_{t,1}, \dots, X_{t,p})'$  denote the  $p$ -dimensional random vector at time  $t$ , for  $t = 1, 2, \dots, n$ . We assume that  $\{\mathbf{X}_t, t = 1, \dots, n\}$  is stationary and ergodic. In addition, we assume that the dependency structure of  $\{\mathbf{X}_t, t = 1, \dots, n\}$  is determined by a DAG  $\mathcal{G}$  with time-order constraint. Here a DAG is defined as  $\mathcal{G} = (A, E)$ , while  $A$  is a finite set of nodes, and  $E$  is a set of directed edges on  $A$ , with no directed cycle. These directed edges in  $\mathcal{G}$  may involve variables at the same time points or between dif-



denote the children, and let  $\text{PCD}[u]$  denote a set that contains  $\text{PC}[u]$  and may contain some descendants of  $u$ . For a subset  $B \subset A$  of the vertices of  $\mathcal{G}$ , the induced subgraph on  $B$  is  $\mathcal{G}[B] := (B, E[B])$ , where  $E[B] := E \cap (B \times B)$ . A  $v$ -structure (also called immorality by, for example, Lauritzen, 1996) is an induced subgraph of  $G$  of the form  $a \rightarrow b \leftarrow c$ . The existence of a  $v$ -structure among a set of three variables can be determined by conditional independence tests (Lauritzen, 1996). The skeleton of a DAG  $\mathcal{G}$  is the undirected graph  $\mathcal{G}^u := (A, E^u)$ ,  $E^u := \{(a, b) \in A \times A \mid a \rightarrow b \text{ or } b \rightarrow a \in \mathcal{G}\}$ . Two DAGs are called Markov equivalent if they induce the same conditional independence restrictions. Two DAGs are Markov equivalent if and only if they have the same global skeleton and the same set of  $v$ -structures (Verma and Pearl, 1990). An equivalence class of DAGs consists of all DAGs that are Markov equivalent. Finally, throughout this paper, we use lower case single letters to present the nodes of the graph unless otherwise specified.

*2.2. A brief review of the Max-Min Parents and Children algorithm.* Our algorithm depends on finding the PCD of a given node  $u$ ,  $\text{PCD}[u]$ . The Max-Min parents and children (MMPC) algorithm originally proposed in Tsamardinos, Aliferis and Statnikov (2003) presents a computationally feasible algorithm to find  $\text{PCD}[u]$  for a given node  $u$  and can be efficiently applied to thousands of variables. The algorithm was further studied and justified by Tsamardinos, Brown and Aliferis (2006). MMPC run on target node  $u$  provides a way to identify the existence of edges to and from  $u$  (but without being able to identify the orientation of the edges). It is a two-phase algorithm. In phase I, the forward phase, variables enter the candidate set of  $\text{PCD}[u]$  sequentially, called CPCD by using the Max-Min heuristic: in each iteration, select the variable that maximizes the minimum association with  $u$  relative to CPCD, and add it to CPCD; the iteration stops when the maximum is zero, i.e. all remaining variables are independent of the target  $u$  given some subset of CPCD. Here the minimum association between  $u$  and  $v$  is the minimum of association between these two variables achieved over all subsets of CPCD. In phase II, the backward phase, the false positives in CPCD, which are independent of  $u$  given a subset of CPCD, are removed from CPCD. This is achieved by testing the conditional independence between  $u$  and  $v$  given some subset of CPCD, if the null is not rejected,  $v$  is removed from CPCD.

*2.3. Algorithm for learning local structure around a target  $T$ .* We extend the PCD-PCD algorithm of Zhou et al. (2010) for local directed graph learning to MTS data by assuming that if there is a link between the variables at different time points, the causal direction is determined and is from the

variable measured at the early time point to the variable measured at the later time point. Like the PCD-PCD algorithm, we first find parents, children and some descendants of the target  $T$  to obtain a local skeleton with a radius of 1, and then repeatedly find PCDs of nodes that are in the previous PCDs and also on the same time point as the target node  $T$ , until the radius of the local skeleton within time point  $t$  is up to the given depth  $d$ . In order to orient the edges in the local skeleton, sometimes it is necessary to find the PCDs further away from the target along some but not all the paths. Note that some of the undirected edges cannot be oriented from the observational data due to the existence of equivalent class (Andersson, Madigan and Perlman, 1997). Zhou et al. (2010) proposed a stopping rule so that the process of finding PCDs can stop early even if some edges within the local graph are not oriented. The stopping rule is based on the fact that when the unoriented edges are surrounded by directed edges, they cannot be oriented by finding further structures.

Our algorithm is divided into two parts. Part I involves finding the local structure around the target  $T$  to the depth of  $d-1$  and Part II finds the edges at the last layer  $d$  and orients undirected edges within the local structure with depth  $d$ . In both parts of the algorithm, we use the index set  $1 : p(q+1)$  to denote the node set  $(\mathbf{X}'_{t-q}, \mathbf{X}'_{t-1}, \dots, \mathbf{X}'_t)'$ , which is ordered according to the time order. Based on this notation, the nodes in  $\mathbf{X}'_t$  are denoted as  $(pq+1) : p(q+1)$  and the target  $T$  is coded with a number in  $(pq+1) : p(q+1)$ . Further more, we use  $V$  to denote a set of variables whose PCDs have been obtained,  $L[i]$  to denote the node set on the  $i$ th layer of the local graph,  $L$  to denote the set of nodes in all layers. In addition, we use  $C[i]$  to denote an ordinal waiting list for layer  $i$  whose PCD is to be determined and  $C$  to denote all the nodes at the current time point. Finally, let  $D$  be the counter of depth of the graph.

Part I of the algorithm is detailed in Table 1. Part I stops if all nodes with a path to  $T$  have a distance shorter than  $d$  or the first  $d-1$  layers of nodes around  $T$  have been obtained. A detailed explanation of the steps of this part of the algorithm can be found as part of the proof of Theorem 1 presented below.

When  $d > 1$ , Part II of the algorithm is required to identify the edges at the last layer  $d$  and to orient the undirected edges within the local structure with depth  $d$ . In Part II, we use the notation

$$\text{struct}(\text{'leaf'}, v, \text{'length'}, l, \text{'path'}, u)$$

to define a set with three different elements, 'leaf' ( $v$ ), 'length' ( $l$ ) and 'path' ( $u$ ), where a 'leaf' is a node  $v$  at layer  $\geq d$ , 'path'  $u$  is a set of variables

TABLE 1

*tsPCD-PCD Algorithm, Part I: find edges within depth  $d - 1$  from the target node  $T$ .*

---



---

1	<b>Initialization:</b> Find the PCD of $T$ , $\text{PCD}[T]$ . $V = \{T\}$ , $L[0] = \{T\}$ , $L(i) = \emptyset$ for $i = 1, \dots, d$ , $L = \{T\}$ , $D = 1$ , $C[0] = \{T\}$ , $C[1] = \text{PCD}[T]$ , $C = (p * q + 1) : p * (q + 1)$ , create directed edges $(\text{PCD}[T] \setminus C \rightarrow T)$ , $C(1) = \text{PCD}[T] \cap C$ .
	<b>Repeat</b>
2	Remove $x$ from the head of list $C[D]$ .
3	If $x \notin V$ , then Find $\text{PCD}[x]$ , and set $V = V \cup x$ . create directed edges $(\text{PCD}[x] \setminus C \rightarrow x)$ $\text{PCD}[x] = \text{PCD}[x] \cap C$ For each $y \in V$ , if $\{x \in \text{PCD}[y] \text{ and } y \in \text{PCD}[x]\}$ , then create an undirected edge $(x, y)$ . Find $v$ -structures for the triple of $x$ , one of $\text{Pa}[x]$ on previous time points and one of nodes on current time point that have undirected edges with $x$ , if $x$ is not in the separator set of the last two nodes. Find $v$ -structures within $V$ including $x$ : {Within $V$ , find possible $v$ -structures only for the triple of $x$ and other two variables in $V$ if an intermediate node is not in the separator set of two nonadjacent nodes.} Orient undirected edges under Meek's rules (Meek, 1995): {Orient other edges between nodes in $V$ if each opposite of them creates either a directed cycle or a new $v$ -structure.} End if
4	If $x \notin L$ and $x \notin L[D]$ and $x$ is adjacent to a node in $L[D - 1]$ then $L[D] = L[D] \cup \{x\}$ and add $(\text{PCD}[x] \cap C) \setminus L$ to the tail of list $C[D + 1]$ . End if.
5	If $C[D] = \emptyset$ then $L = L \cup L[D]$ and $D = D + 1$ End if.
6	<b>Until</b> $C[D] = \emptyset$ or $D \geq d$ .

---



---

on the path from layer  $d - 1$  to the ‘leaf’  $v$  and ‘length’ is the length from layer  $d - 1$  to ‘leaf’  $v$ . For a given element  $x$  in this set,  $x.leaf$ ,  $x.path$  and  $x.length$  denote the three elements of the list, respectively. Details of Part II of the tsPCD-PCD algorithm are given in Table 2. A detailed explanation of the steps of Part II can be found as part of the proof of Theorem 1.

TABLE 2

*tsPCD-PCD Algorithm, Part II: find edges at layer  $d$  and orient undirected edges within the local structure.*

---



---

1	<b>Initialization:</b> Learn the PCDs of nodes at the layer $d-1$ , and construct a set $W$ : $W = \{struct('leaf', v, 'length', 1, 'path', u) : u \in L[d - 1], v \in (PCD[u] \cap C) \setminus L\}$ <b>Repeat</b>
2	Remove $x$ from the head of list $W$ .
3	If all edges on path $x.path$ are undirected then If $x.leaf \notin V$ then Find $PCD[x.leaf]$ and set $V = V \cup \{x.leaf\}$ . Create directed edges $(PCD[x.leaf] \setminus C \rightarrow x.leaf)$ $PCD[x.leaf] = PCD[x.leaf] \cap C$ For each $y \in V$ , if $\{x.leaf \in PCD(Y) \text{ and } y \in PCD[x.leaf]\}$ , create an undirected edge $(x.leaf, y)$ . Find $v$ -structures for the triple of $x.leaf$ , one of $Pa[x.leaf]$ on previous time points and one of nodes on current time point that have undirected edges with $x.leaf$ , if $x.leaf$ is not in the separator set of the last two nodes. Find $v$ -structures within $V$ including $x.leaf$ . Orient undirected edges under the Meek’s rules (Meek, 1995). End if. If there is an undirect edge between $x.leaf$ and the last node $u$ of $x.path$ , then add $struct('leaf', v, 'length', x.length + 1, 'path', [x.path, x.leaf]) :$ $v \in PCD[x.leaf] \cap C \setminus x.path \setminus L \}$ to the tail of $W$ . End if.
4	<b>Until</b> $W = \emptyset$ . Return

---



---

The following theorem shows the effectiveness of the algorithm for recovering the true directed local graph structure for the Markov equivalence class of the underlying global DAG.

**THEOREM 1.** *Suppose that a DAG is faithful to the probability distribution  $P$  of the multivariate time series  $\mathbf{X}_t$  and all conditional independencies can be correctly inferred based on the data. Then for a given target node  $T$ ,*

the *tsPCD-PCD* algorithm can correctly recover the edges within a depth  $d$  of the local directed graphical structure around  $T$  at the same time point and the edges connecting  $T$  and the variables on previous time points. Furthermore, the algorithm obtains the same orientations of these edges as a partially directed graph for the Markov equivalence class of the underlying global DAG.

The proof of this theorem, which is based on detailed explanations of the steps of the algorithm, is given in Online Supplemental Material.

2.4. *An illustrative example.* As a simple illustration of the algorithm, we consider the ALARM network structure as shown in Figure 1(a) (Beinlich et al., 1989) with 37 nodes and 46 edges. This ALARM DAG has been extensively used in evaluating DAG learning algorithms. We extend this network to a dynamic DAG depicting stationary time series with lag  $q = 1$  by assuming that each variable is also influenced by itself on the previous time point. We aim to identify the local network of node 20 to depth  $d = 2$ . We choose node 20 since it has the largest degrees among all the nodes. Suppose that the data are large enough to correctly identify all the required conditional independence. Figure 1 (b) shows a local network with  $d = 1$  that is determined by Part I of the algorithm and Figure 1 (c) shows the final local network with  $d = 2$  after applying Part II of the algorithm. Note that there is no guarantee that all edges can be oriented by the algorithm. If there are some unoriented edges, we need to extend the network along the undirected paths in order to orient those undirected edges in Part II. In this example, since all edges are oriented after learning the first two layers, the algorithm stops extending to higher layers.

To illustrate Part II, in the initialization step, we construct the set  $W$ , which contains the potential undirected edges that may need to be extended to higher layers for edge orientation within first  $d = 2$  layers. For a give node  $x_{t,18} \in L[1]$ , we have  $\text{PCD}[x_{t,18}] = \{x_{t-1,18}, x_{t,14}, x_{t,15}, x_{t,16}, x_{t,20}\}$ . Since  $x_{t-1,18} \rightarrow x_{t,18}$  and  $\{x_{t,20}, x_{t,16}\} \in L[0] \cup L[1]$ , these three nodes are not used as leafs in constructing the set  $W$ . We then add

$$\text{struct}(\text{'leaf'}, x_{t,14}, \text{'length'}, 1, \text{'path'}, x_{t,18})$$

and

$$\text{struct}(\text{'leaf'}, x_{t,15}, \text{'length'}, 1, \text{'path'}, x_{t,18})$$

to  $W$  for node  $x_{t,18} \in L[1]$ . Similarly, we add other elements to  $W$  for each of the other nodes in  $L[1]$  and finish the initialization of  $W$ .

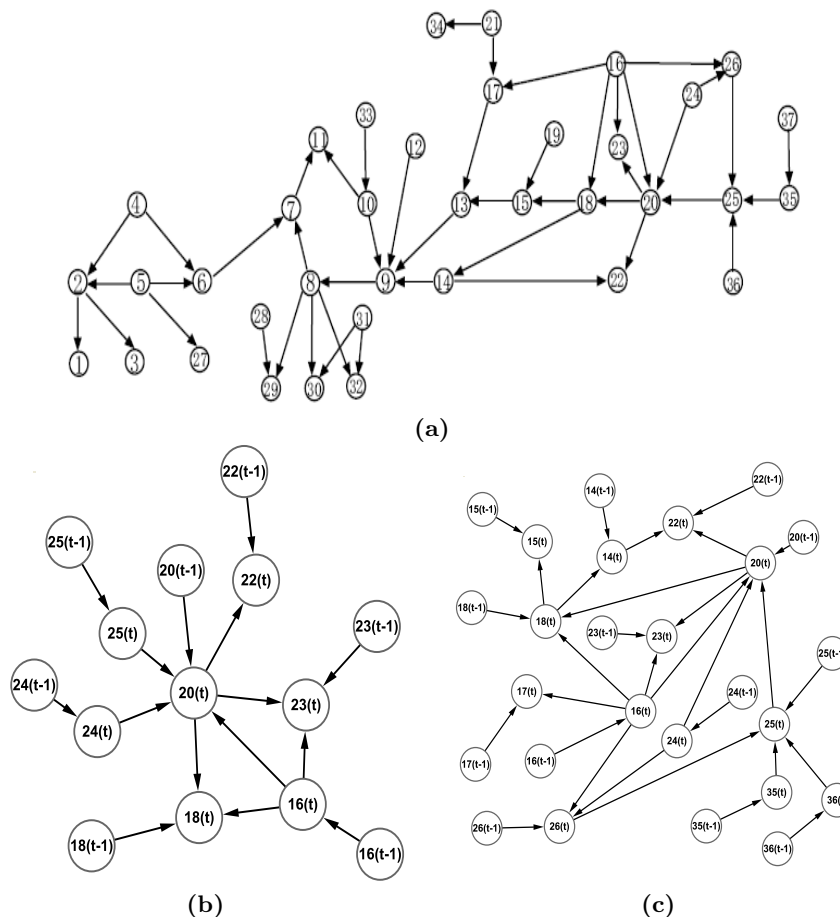


FIG 1. (a) The DAG used in simulations for variables on the same time point; (b) Local network around node 20 learned by Part I of the algorithm; (c) Local network around node 20 learned by Part II of the algorithm.

**3. Composite Likelihood Ratio Tests for Conditional Independence.** The tsPCD-PCD algorithm and also the validity of Theorem 1 depends on a valid and powerful test for conditional dependency. Specifically, finding the PCD of a node using the MMPC algorithm and finding the  $v$ -structures among a set of three variables both rely on testing for conditional independence. For the time series data, since the data across different time points are dependent, the commonly used LRTs tests cannot be applied directly. We propose to develop composite likelihood ratio tests for conditional independence and derive their asymptotic distributions.

3.1. *The composite likelihood ratio tests for general parametric models.* Consider a model for the joint density of  $\mathbf{X} = (\mathbf{X}'_{t-q}, \dots, \mathbf{X}'_t)$ , denoted by  $P(\mathbf{X}'_{t-q}, \dots, \mathbf{X}'_t; \theta)$ , where  $\theta \in \mathcal{H} \subseteq \mathbb{R}^k$  is a  $k$ -dimensional model parameter, where  $\mathcal{H}$  is an open set. The conditional independence test is used in our algorithm for determining the PCDs and  $v$ -structures. Depending on the models assumed, the null model under the conditional independence assumption corresponds to certain constraints on the model parameter  $\theta$ , i.e.,  $h(\theta) = 0$  for some multidimensional function  $h$  (see Lemma 2, Supplemental Materials). If the first-order partial derivative of  $h$  is continuous, it can be equivalently expressed as  $\theta = g(\varphi)$ , where  $\varphi$  is a parameter vector with dimension lower than  $k$ . As an example, consider a joint multivariate model with four variables  $X_1, X_2, X_3$ , and  $X_4$ , with a joint density  $\mathcal{N}(0, \Sigma)$ , where  $\Sigma = (\sigma_{ij})$  is a  $4 \times 4$  matrix. Under this simple model,

$$H_0 : X_1 \perp X_2 | X_3 \Leftrightarrow H_0 : \Sigma_{X_1, X_2, X_3}^{-1}(1, 2) = 0 \Leftrightarrow H_0 : \sigma_{12} = \frac{\sigma_{13} * \sigma_{23}}{\sigma_{33}}.$$

Similarly, for categorical variables and log-linear models, the null hypothesis of conditional independence corresponds to constraints on model parameters (Lauritzen, 1996). We therefore consider the conditional independence null hypothesis that can be expressed as

$$(1) \quad H_0 : \theta = g(\varphi),$$

where  $\theta \in \mathbb{R}^k$ ,  $\varphi \in \mathbb{R}^{k-r}$  and  $g: \mathbb{R}^{k-r} \rightarrow \mathbb{R}^k$  is a function with  $\frac{\partial}{\partial \varphi} g(\varphi)$  being of full rank. Under the conditional independence null hypothesis, the parameter can be written as  $\mathcal{H}_0 = \{\theta : \theta = g(\varphi)\}$ .

For multiple time series  $\{\mathbf{X}_t^{(j)}, t = 1, \dots, n_j, j = 1, \dots, m\}$ , we propose the following composite likelihood ratio test statistic  $G_{CLRT}^2$  for testing the null hypothesis (1) defined as

$$G_{CLRT}^2 = -2 \log \frac{\sup_{\mathcal{H}_0} \prod_{j=1}^m \prod_{t=q+1}^{n_j} P\{\mathbf{X}_{t-q}^{(j)}, \mathbf{X}_{t-q+1}^{(j)}, \dots, \mathbf{X}_t^{(j)}; \theta = g(\varphi)\}}{\sup_{\mathcal{H}} \prod_{j=1}^m \prod_{t=q+1}^{n_j} P(\mathbf{X}_{t-q}^{(j)}, \mathbf{X}_{t-q+1}^{(j)}, \dots, \mathbf{X}_t^{(j)}; \theta)},$$

which is the likelihood ratio statistic based on the piled data treating the data as independent. Because of the dependency of the data, the null distribution of the statistic  $G_{CLRT}^2$  is not the standard  $\chi_r^2$  distribution.

Denote  $\theta_0$  as the true value of  $\theta$  under the null  $H_0$  and  $\varphi_0$  as the corresponding  $\varphi$ , i.e.,  $\theta_0 = g(\varphi_0)$ . Define the  $k$ -dimensional column vector

$$\mathbf{Z}_t = \frac{\partial}{\partial \theta} \log P(\mathbf{X}_{t-q}, \mathbf{X}_{t-q+1}, \dots, \mathbf{X}_t; \theta)|_{\theta=\theta_0},$$

which is a stationary ergodic sequence. Let  $\mathbf{Z}_t^{(j)}$  be the corresponding sample value for  $j = 1, \dots, m$ . Assuming the standard regularity conditions on the joint probability density function  $P(\mathbf{X}_{t-q}^{(j)}, \mathbf{X}_{t-q+1}^{(j)}, \dots, \mathbf{X}_t^{(j)}; \theta)$  as commonly assumed for the likelihood ratio test statistics (Cox and Hinkley, 1979), Theorem 2 in the Online Supplemental Material, for the case of a long time series and few replications, shows that the asymptotic distribution of the CLRT statistic  $G_{CLRG}^2$  follows a mixture of  $\chi^2$  distributions, not a simple  $\chi^2$  distribution as with conventional LRT statistics. Theorem 3 shows a similar result when  $m \rightarrow \infty$  and  $n_j = n$  for all  $j$ , i.e., a short time series with many replications. The exact statements of both Theorems and their proofs can be found in the Online Supplemental Material.

*3.2. Conditional independence tests for the Gaussian DAG models.* In this section, we consider the Gaussian DAGs for continuous random variables. In the MTS setting, we assume that  $(\mathbf{X}'_{t-q}, \dots, \mathbf{X}'_{t-1}, \mathbf{X}'_t)'$  follows a multivariate normal distribution  $N(0, \Sigma)$  where the DAG determines the local dependency structures of the variables and the therefore corresponding covariance matrix  $\Sigma$ . In our tsPCD-PCD algorithm, the tests for conditional independence can be written as  $H_0 : X_{t,a} \perp X_{t-l,b} | S_{t,q}$ , where  $\{X_{t,a}, X_{t-l,b}, S_{t,q}\} \subseteq A = \{\mathbf{X}'_{t-q}, \dots, \mathbf{X}'_{t-1}, \mathbf{X}'_t\}$  with  $0 \leq l \leq q$  and  $a, b \in \{1, \dots, p\}$ , and  $S_{t,q}$  is a separator set. The corresponding CLRT statistic can be written as

$$G_{CLRT}^2 = -2 \log \frac{\sup_{\mathcal{H}_0} \prod_{j=1}^m \prod_{t=q+1}^{n_j} P(X_{t,a}^{(j)}, X_{t-l,b}^{(j)}, S_{t,q}^{(j)}; \theta = g(\phi))}{\sup_{\mathcal{H}} \prod_{j=1}^m \prod_{t=q+1}^{n_j} P(X_{t,a}^{(j)}, X_{t-l,b}^{(j)}, S_{t,q}^{(j)}; \theta)}.$$

Corollary 1 in the Online Supplemental Material shows that under the Gaussian DAG model and the null hypothesis  $H_0 : X_{t,a} \perp X_{t-l,b} | S_{t,q}$ ,  $G_{CLRT}^2 / \hat{\lambda}$  follows a  $\chi_1^2$  distribution, where the exact expression of  $\hat{\lambda}$  can also be found.

**4. Simulation Studies.** In this section we evaluate the performance of the tsPCD-PCD algorithm in learning the local directed graphical structure. We consider the dynamic graph (Figure 1 (a)) used in Section 2.4 with time series data of lag 1. For each simulation, we simulate a training data set from a joint Gaussian distribution using a structural equation model of recursive linear regressions derived from the assumed DAG structure with residual variances of 1. The regression coefficients are randomly generated uniformly from  $(-0.6, -0.2) \cup (0.2, 0.6)$  or from  $(-0.6, -0.4) \cup (0.4, 0.6)$ . We consider models with different sample sizes and both data from one long time series and data from multiple short time series. These parameters were chosen to

give reasonable signal-to-noise ratios for the given sample sizes. We repeat the simulations 100 times and obtain the average values of the performance scores for each case.

Similar to the example in Section 2.4, our goal is to obtain the local graph around the node  $T = 20$  at the depth  $d = 1$ . In the true graph, node 20 connects with many other nodes and has the largest degree.

4.1. *Validity of the CLRT statistic.* We first demonstrate that the CLRT statistic  $G_{CLRT}^2$  does not follow the standard  $\chi^2$ -distribution and instead it follows a re-scaled  $\chi^2$  distribution. We consider two null hypotheses  $H'_0 : X_{t,24} \perp X_{t,2}$  and  $H''_0 : X_{t,4} \perp X_{t,1} | \{X_{t-1,2}, X_{t,2}\}$  in model of one single time series of length  $n = 500$  and the regression coefficients being generated uniformly from  $(-0.6, -0.4) \cup (0.4, 0.6)$ . For  $H'_0$  and  $H''_0$ ,  $\lambda$  is around 1.8 and 1.2, respectively. We can see from the Q-Q plots over 1000 simulations in Figure 2 that the CLRT statistic  $G_{CLRT}^2$  greatly deviates from  $\chi_1^2$ , while the re-scaled statistic  $G_1^2/\hat{\lambda} \rightarrow \chi_1^2$ , which indicates that the asymptotic result of the CLRT statistic holds.

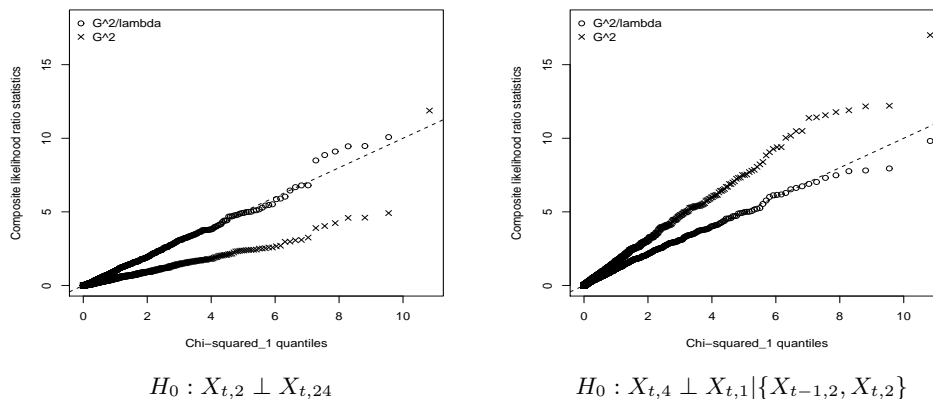


FIG 2. *Distribution of the CLRT statistic under two null hypotheses based on the simulated data, demonstrating that the CLRT statistic follows a re-scaled  $\chi_1^2$  distribution.*

4.2. *Performance in recovering the local directed graph.* To evaluate the performance of tsPCD-PCD in recovering the local directed graphical structure, for each of three subsets: parents (Pa), children (Ch) and all depth 1 variables (PC), we calculate the score pair (precision, recall), where Preci-

sion and Recall or sensitivity are defined as:

$$\text{precision} = \frac{\text{no. of true positives}}{\text{no. of edges identified}}, \quad \text{recall} = \frac{\text{no. of true positives}}{\text{no. of true edges}}.$$

Table 3 shows the precision and recall results for four different models when different test statistics with significance level  $\alpha = 0.01$  for the conditional independence tests are used. Overall, we observe that the set PC(20) can be identified very well in all four models. In addition, multiple time series resulted in similar results as single time series when the total number of observations are comparable. Second, the CLRTs using the correct null distribution (i.e., mixture of  $\chi^2$ -distributions) gave better performances than that using the wrong null distributions in both precision and recall, especially when the average cross-time correlations are high or when the sample sizes are large. Almost identical results are observed when the significance level is set to  $\alpha = 0.005$ .

TABLE 3

*Precision and recall of the local DAG graph around node 20 in the DAG shown in Figure 1 (a) based on 100 replications using tsPCD-PCD or PCD-PCD algorithm. The composite likelihood ratio tests are used for testing the conditional independence with  $\alpha = 0.01$  with/without including the re-scaling factor  $\hat{\lambda}$  to adjust for the dependency of the observations.*

Statistic	Method	Precision			Recall		
		Pa	Ch	PC	Pa	Ch	PC
$n = 500, M = 1, \beta \in (-0.6, -0.2) \cup (0.2, 0.6)$							
$G_{CLRT}^2$	tsPCD-PCD	0.50	0.82	0.97	0.44	0.47	0.73
	PCD-PCD	0.37	0.60	1.00	0.16	0.64	0.70
$G_{CLRT}^2/\hat{\lambda}$	tsPCD-PCD	0.55	0.82	0.98	0.41	0.59	0.72
	PCD-PCD	0.35	0.58	1.00	0.16	0.61	0.71
$n = 10, M = 50, \beta \in (-0.6, -0.2) \cup (0.2, 0.6)$							
$G_{CLRT}^2$	tsPCD-PCD	0.50	0.83	0.97	0.43	0.47	0.72
	PCD-PCD	0.41	0.62	1.00	0.16	0.69	0.70
$G_{CLRT}^2/\hat{\lambda}$	tsPCD-PCD	0.53	0.83	0.97	0.42	0.55	0.71
	PCD-PCD	0.41	0.63	1.00	0.19	0.64	0.70
$n = 500, M = 1, \beta \in (-0.6, -0.4) \cup (0.4, 0.6)$							
$G_{CLRT}^2$	tsPCD-PCD	0.42	0.91	0.90	0.27	0.64	0.60
	PCD-PCD	0.26	0.69	1.00	0.10	0.60	0.59
$G_{CLRT}^2/\hat{\lambda}$	tsPCD-PCD	0.84	0.95	0.99	0.32	0.87	0.61
	PCD-PCD	0.32	0.68	1.00	0.14	0.56	0.59
$n = 1000, M = 1, \beta \in (-0.6, -0.2) \cup (0.2, 0.6)$							
$G_{CLRT}^2$	tsPCD-PCD	0.35	0.82	0.82	0.25	0.70	0.64
	PCD-PCD	0.29	0.67	0.99	0.12	0.63	0.63
$G_{CLRT}^2/\hat{\lambda}$	tsPCD-PCD	0.94	0.88	1.00	0.33	0.95	0.66
	PCD-PCD	0.30	0.62	1.00	0.13	0.59	0.64

4.3. *Improved performance when time order is used.* We finally demonstrate that by using the time order information to orient the edges, we can substantially increase both the precision and recall rates for the parents and children sets. Table 3 also shows the precision and recall results from the standard PCD-PCD algorithm that ignores the time series nature of the data for the same sets of models. We observe clear decreases in both precisions and recalls for the parents and children sets of a node when the time order information is ignored, while the selections of all depth 1 variables are comparable. The results clearly indicate the tsPCD-PCD algorithm that utilizes the time order to orient the edges can lead to better identification of the parents and children nodes of a target variable.

**5. Application to a Real Data Set.** The central event in the generation of a cellular immune response to stimulants is the activation of T-cells. T-cell activation is initiated by the interaction between the T-cell receptor complex and the antigenic peptide presented on the surface of the cells. Such an activation triggers a network of proteins, kinases, phosphatases and adaptor proteins that lead to gene transcription events in the nucleus, including transcription of a number of transcription factors such as c-Fos, c-myc, c-jun and activation of early genes such as such as interleukins (e.g. IL2, IL3R etc). These genes in turn induce the expression of a number of effector genes. Days after the activation event, various adhesion molecules begin to be expressed. It is therefore very important to understand the causal relationships among the genes involved in T-cell activation.

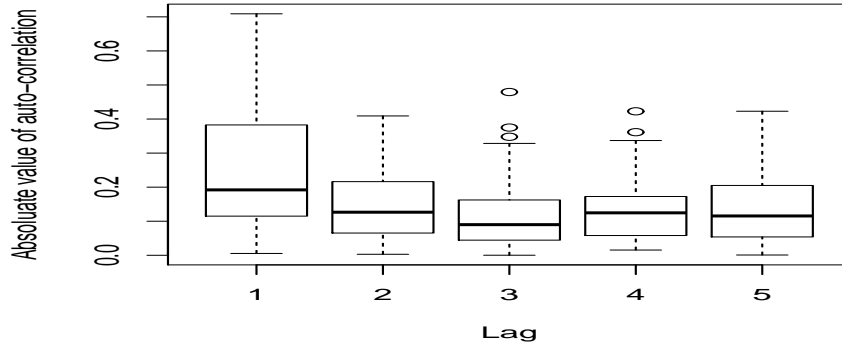
Rangel et al. (2004) measured gene expression levels of  $p = 58$  genes that are related to T-cell activation over  $n = 10$  time points (0, 2, 4, 6, 8, 18, 24, 32, 48, 72 hours) after treating the T-cells with ionomycin. Expression data over  $m = 44$  biological replications were obtained. Following Rangel et al. (2004); Rau et al. (2010), we log-transformed the expression data and performed the quantile normalization (Bolstad et al., 2002) to ensure that all 44 replicates have a similar underlying distribution of gene expression. The normalized expression data and gene descriptions can be found in the R package GeneNet of (Schäfer, Opgen-Rhein and Strimmer, 2006) on CRAN (R Development Core Team, 2009).

Instead of learning the whole gene regulatory network among these 58 genes related to Jurket T-cell activation, we focused on learning the local directed graphs of three important genes (Rangel et al., 2004; Rau et al., 2010), including the transcription factors JunB, JunD and FYB genes using the proposed tsPCD-PCD algorithm. JunB and c-Jun, along with JunD and Fos group proteins (c-fos, FosB, Fra1, and Fra2), comprise the core members

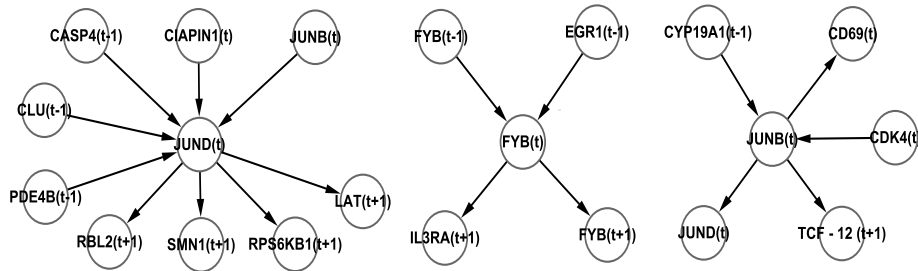
of the activator protein 1 (AP1) family of transcription factors. Since the time series we have are very short with  $n = 10$ , following Rau et al. (2010) and Rangel et al. (2004), we assume a lag  $q = 1$  under a Gaussian model to learn local networks around these three genes separately. Choosing  $q = 1$  is partially justified by the boxplots of the auto-correlations for different lag sizes shown in Figure 3 (a). The auto-correlations are small for lags greater than 1. We used the significance level of  $\alpha = 0.01$  for all the conditional independence tests based on the CLRTs or LRTs.

Figure 3 (b) shows the local neighbors identified by the tsPCD-PCD method for each of the three genes. We first observe that genes JunB and JunD have more neighbors than FYB gene, showing the importance of these two genes in T-cell activation (Boise et al., 1993). Out of the five genes that are found to regulate expression of JunD (CIAPIN, CLU, CASP, PDE4B and JunB), three are related to apoptosis, including the cytokine-induced inhibitor of apoptosis (CIAPIN) and the clusterin (CLU) genes that are associated with the clearance of cellular debris and apoptosis, and apoptosis-related cycteine peptide (CASP). This is very interesting since the T-cells were stimulated by the calcium ionophore ionomucin, which is known to induce apoptosis (Miyake et al., 1999) by activating the apoptosis-related genes. These apoptosis events then lead to activation of JunD, which in term regulates genes of survival of motor neuron 1 (SMN1), ribosomal protein kinase S6 (RPS6Kb1), retinoblastoma like protein 2 (RBL2) and linker gene for activation of T-cells (LAT), all at the next time point. This observation agrees with the known fact that JunD mediates survival signaling to mount an appropriate biological response to a specific challenge (Lamb et al., 2003). Among these genes, LAT plays an important role in the activation, homeostasis and regulatory function of T cells (Shen et al., 2010) and RBL2 is a key regulator of entry into cell division and survival. The ribosomal protein S6 kinase (RPS6K1) is a central regulator of protein synthesis and of cell proliferation, differentiation and survival (Han, Khuri and Roman, 2006). This example shows the effectiveness of our methods in identifying the upstream regulators and downstream regulated genes of JunD during T-cell activation. This is in contrast to the global network identified by Rau et al. (2010) using a state-space model, where only Caspase-4 was identified as the upstream regulator of JunD.

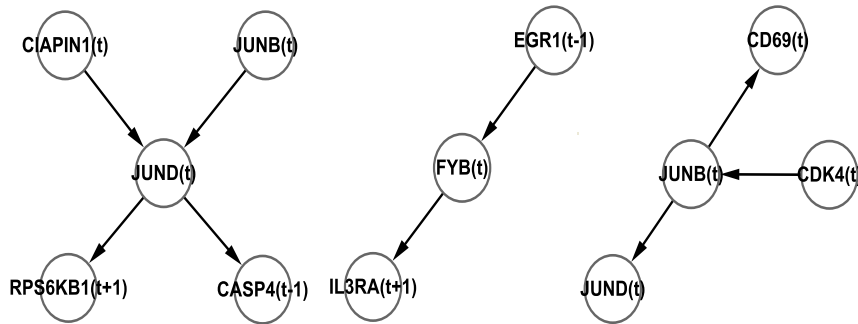
JunB is a cell cycle-regulated transcription factor this is involved in the regulation of a broad spectrum of cellular functions, including the expression of leukocyte early activation antigen CD69 (Castellanos et al., 1997). It also interacts with JunD. tsPCD-PCD identifies these two genes as the downstream targets of JunB. Cyclin-dependent kinases (CDK4) and their



(a) Boxplots of the absolute values of the autocorrelations of 58 genes.



(b) Local networks learned using the tsPCD-PCD algorithm.



(c) Local networks learned using the PCD-PCD algorithm.

FIG 3. Analysis of real data set: boxplots and local structures learned around genes  $JUND$ ,  $FYB$  and  $JUNB$  based on time course gene expression data using the significant level  $\alpha = 0.01$  and depth = 1.

targets have been primarily associated with regulation of cell-cycle progression. Vanden Bush and Bishop (2011) recently identified JunB as a newly recognized CDK substrate, supporting the fact that CDK4 is a upstream regulator of JunB. Our method also identifies CYP19A as another potential regulator of JunB.

Finally, the early-growth response 1 (EGR-1) transcription regulator was first identified as an immediate-early response gene transcriptionally activated by mitogenic stimulation (Sukhatme et al., 1988). It regulates FYN binding protein (FYB), which is an important adaptor molecule in the T-cell receptor signaling machinery that in turn influences the expression of interleukin 3 receptor,  $\alpha$  (IL3RA). These results agree with the current literature. In contrast, in work by Rangel et al. (2004), FYB was found to occupy a crucial position in the graph and was involved in the highest number of outward connections. However, our local DAG does not support this conclusion. It is also interesting to see that FYB tends to self-regulate over time as shown by the identified edges  $FYB(t-1) \rightarrow FYB(t) \rightarrow FYB(t+1)$ .

As a comparison, we also applied the PCD-PCD algorithm that ignores the time series nature of the data and show the resulting local networks in Figure 3 (b). Ignoring the time dependency leads to less well-connected graphs compared with the ones obtained by tsPCD-PCD. For example, important apoptosis related JunD regulators CLU and CASP were not identified by the PCD-PCD algorithm. This indicates that our algorithm is able to extract additional information about the interactions among the investigated genes based on the time-course gene expression data.

**6. Discussion.** Motivated by analysis of time course gene expression data with replicates, we have developed a learning algorithm to identify the neighboring nodes of a given variable by extending the PCD-PCD algorithm of Zhou et al. (2010) in order to effectively utilize the time-order in orienting the edges. Like many constraint-based methods, our algorithm depends on valid tests for conditional independence. To account for the dependency among the observations in time series data, we developed composite likelihood ratio tests that provide valid tests for conditional independence for general parametric DAG models, including the log-linear and the Gaussian DAG models. While there are other alternative tests for continuous variables without assuming a functional form between the variables as well as the data distributions such as the kernel-based tests (Zhang et al., 2012), it is not clear how to extend these tests to the multivariate time series data in the context of learning the DAGs.

Theorem 1 of this paper shows that the proposed tsPCD-PCD algorithm

can recover the true local DAG (up to a Markov equivalent class) if the DAG is faithful to the joint probability distribution and if all the conditional independence conditions can be correctly checked with the data. Therefore, the power of discovering the true local network depends on the power and type 1 error of the conditional independence tests. However, since many such conditional independence tests are performed in the algorithm, it does not seem to be possible to develop a general framework to determine the sample sizes needed in order to recover the true DAG with a high probability. This is an interesting topic for future research.

In our analysis of the gene expression data, the tsPCD-PCD algorithm has identified several important regulatory relationships among the genes in T-cell activation pathways, many agree with our current knowledge on T-cell activation. The fact that many edges identified by our method can be substantiated by literature shows its effectiveness in identifying biologically useful information on gene regulation. As a necessary simplification, we assume that DAG structure is time-invariant. When data are collected over many time points and with many replications such as those measured at single-cell levels, it is possible to extend our methods for studying time-dependent DAG structures that can reflect the dynamic changes of the DAG structures.

**Acknowledgements.** We thank You Zhou and Changzhang Wang for sharing their source codes for PCD-PCD algorithm. Wanlu Deng’s research is partially funded by the China State Scholarship Fund. We thank Professor Karen Kafadar, the associate editor and the reviewers for very helpful comments and suggestions that have led to great improvement in presentation.

#### SUPPLEMENTARY MATERIAL

##### **Supplemental materials for “Learning Local Directed Acyclic Graphs Based On Multivariate Time Series Data”**

(<http>). The online supplemental materials include detailed statements and their proofs of Theorems 1-3, Lemma 2 and Corollary 1. Proof of Theorem 1 provides detailed explanation of the steps of Part I and Part II of the tsPCD-PCD algorithm.

##### **References.**

- ANDERSSON, S. A., MADIGAN, D. and PERLMAN, M. (1997). A characterization of Markov equivalence classes for acyclic digraphs. *Annals of Statistics* **25** 505–541.
- BEINLICH, I. A., SUERMONDT, H. J., CHAVEZ, R. M. and COOPER, G. F. (1989). The ALARM monitoring system: A case study with two probabilistic inference techniques for belief networks. *Proc. of the Second European Conf. on Artificial Intelligence in Medicine*.

- BOISE, L. H., PETRYNIAK, B., MAO, X., JUNE, C., WANG, C., LINDSTEN, T., BRAVO, R., KOVARY, K., LEIDEN, J. and THOMPSON, C. (1993). The NFAT-1 DNA binding complex in activated T cells contains Fra-1 and JunB. *Molecular and Cellular Biology* **13** 1911–1919.
- BOLSTAD, B., IRIZARRY, R., ASTRAND, M. and SPEED, T. (2002). A comparison of normalization methods for high density oligonucleotide array data based on bias and variance. *Bioinformatics* **19** 185–193.
- BUGANIM, Y., FADDAH, D. A., CHENG, A. W., ITSKOVICH, E., MARKOULAKI, S., GANZ, K., KLEMM, S. L., VAN OUDENAARDEN A., and JAENISCH, R. (2012). Single-cell expression analyses during cellular reprogramming reveal an early stochastic and a late hierarchic phase. *Cell* **150** 1209–1222.
- CASTELLANOS, M. C., MUNOZ, C., MONTOYA, M. C., LARA-PEZZI, E., LOPEZ-CABRERA, M. and DE LANDAZURI, M. O. (1997). Expression of the leukocyte early activation antigen CD69 is regulated by the transcription factor AP-1. *The Journal of Immunology* **159** 5463–5473.
- CHICKERING, D. (2002). Optimal structure identification with greedy search. *Journal of Machine Learning Research* **3** 507–554.
- COOPER, G. and HERSKOVITS, E. (1992). A Bayesian method for the induction of probabilistic networks from data. *Machine Learning* **9** 309–347.
- COX, D. R. and HINKLEY, D. (1979). *Theoretical Statistics*. Chapman & Hall.
- ELLIS, B. and WONG, W. H. (2008). Learning causal Bayesian network structures from experimental data. *Journal of the American Statistical Association* **103** 778–789.
- FRIEDMAN, N. and KOLLER, D. (2003). Being Bayesian about network structure: A Bayesian approach to structure discovery in Bayesian networks. *Machine Learning* **50** 95–126.
- FRIEDMAN, N., LINIAL, M., NACHMAN, I. and PE’ER, D. (2000). Using Bayesian networks to analyze expression data. *Journal of Computational Biology* **7** 601–620.
- GHAHRAMANI, Z. (1997). Learning dynamic Bayesian networks. *Lecture Notes In Computer Science* **1387** 168–197.
- GRZEGORCZYK, M. and HUSMEIER, D. (2011). Improvements in the reconstruction of time-varying gene regulatory networks: dynamic programming and regularization by information sharing among genes. *Bioinformatics* **27** 693–699.
- HAN, S., KHURI, F. R. and ROMAN, J. (2006). Fibronectin stimulates non-small cell lung carcinoma cell growth through activation of Akt/mammalian target of rapamycin/S6 kinase and inactivation of LKB1/AMP-activated protein kinase signal pathways. *Cancer Research* **66** 315–323.
- HECKERMAN, D. (1995). A Tutorial on learning with Bayesian networks.
- HUSMEIER, D. (2003). Sensitivity and specificity of inferring genetic regulatory interactions from microarray experiments with dynamic Bayesian networks. *Bioinformatics* **19** 2271–2282.
- LAMB, J. A., VENTURA, J. J., HESS, P., FLAVELL, R. A. and DAVIS, R. J. (2003). JunD mediates survival signaling by the JNK signal transduction pathway. *Mol. Cell* **11** 1479–89.
- LAURITZEN, S. (1996). *Graphical Models*. Clarendon Press, London.
- LI, H. and GUI, J. (2006). Gradient directed regularization for sparse Gaussian concentration graphs, with applications to inference of genetic networks. *Biostatistics* **7** 302–317.
- LI, S., HSU, L., WANG, P. and PENG, J. (2013). Bootstrap Inference for Network Construction With an Application to a Breast Cancer Microarray Study. *Annals of Applied Statistics* **In press**.
- MARGARITIS, D. and THRUN, S. (2000). Bayesian network induction via local neigh-

- borhoods. In *Advances in Neural Information Processing Systems 12* (S. A. SOLLA, T. K. LEEN and K. R. MÜLLER, eds.) 505–511. MIT Press.
- MEEK, C. (1995). Causal inference and causal explanation with background knowledge. *Proceedings of the 11th Annual Conference on Uncertainty in Artificial Intelligence* **95** 403–418.
- MIYAKE, H., HARA, I., YAMANAKA, K., ARAKAWA, S. and KAMIDONO, S. (1999). Calcium ionophore, ionomycin inhibits growth of human bladder cancer cells both in vitro and in vivo with alteration of Bcl-2 and Bax expression levels. *J Urol.* **162** 916–21.
- MURPHY, K. and MIAN, S. (1999). Modelling gene expression data using dynamic bayesian networks Technical Report, University of California, Berkeley.
- NEAPOLITAN, R. E. (2003). *Learning Bayesian Networks*. Prentice Hall.
- PEARL, J. (2000). *Causality: models, reasoning and inference*. Cambridge University Press, Cambridge.
- RANGEL, C., ANGUS, J., GHARAMANI, Z., LIOUMI, M., SOUTHERAN, E., GAIBA, A., WILD, D. L. and FALCIANI, F. (2004). Modeling T-cell activation using gene expression profiling and state-space model. *Bioinformatics* **20(9)** 1361–1372.
- RAU, A., JAFFREZIC, F., FOULLEY, J. and DOERGE, R. W. (2010). An empirical Bayesian method for estimating biological networks from temporal microarray Data. *Statistical Applications in Genetics and Molecular Biology* **9**.
- SCHÄFER, J., OPGEN-RHEIN, R. and STRIMMER, K. (2006). Reverse engineering genetic networks using the GeneNet package. *R News* **6** 50-53.
- SCHÄFER, J. and STRIMMER, K. (2005). An empirical Bayes approach to inferring large-scale gene association networks. *Bioinformatics* **21** 754–764.
- SHEN, S., CHUCK, M. I., ZHU, M., FULLER, D. M., OU YANG, C. W. and ZHANG, W. (2010). The importance of LAT in the activation, homeostasis, and regulatory function of T cells. *J. Biol. Chem.* **285** 35393–35405.
- SPIRITES, P., GLYMOUR, C. and SCHEINES, R. (2000). *Causation, Prediction, and Search*, second ed. MIT Press, Cambridge, MA.
- SUKHATME, V., CAO, X., CHANG, L., TSAI-MORRIS, C., STAMENKOVICH, D., FERREIRA, P., COHEN, D., EDWARDS, S. A., SHOWS, T., LEBEAU, T. and ADAMSON, E. (1988). A zinc finger-encoding gene coregulated with c-fos during growth and differentiation, and after cellular depolarization. *Cell* **53** 37–43.
- TSAMARDINOS, I., ALIFERIS, C. F. and STATNIKOV, A. (2003). Time and sample efficient discovery of Markov blankets and direct causal relations In *The Ninth ACM SIGKDD International Conference on Knowledge Discovery and Data Mining* 673–678.
- TSAMARDINOS, I., BROWN, L. E. and ALIFERIS, C. F. (2006). The max-min hill-climbing Bayesian network structure learning algorithm. *Machine Learning* **65** 31–78.
- VANDEN BUSH, T. J. and BISHOP, G. A. (2011). CDK-Mediated regulation of cell functions via c-Jun phosphorylation and AP-1 activation. *PLoS ONE* **6(4)** e19468.
- VERMA, T. and PEARL, J. (1990). Equivalence and synthesis of causal models. In *Proceedings of the Sixth Annual Conference on Uncertainty in Artificial Intelligence* 255-268.
- YIN, J., ZHOU, Y., WANG, C., HE, P., ZHENG, C. and GENG, Z. (2008). Partial orientation and local structural learning of causal networks for prediction. *JMLR: Workshop and Conference Proceedings* **3** 93–104.
- ZHANG, K., PETERS, J., JANZING, D. and SCHOELKOPF, B. (2012). Kernel-based conditional independence test and application in causal discovery Technical Report.
- ZHOU, Y., WANG, C., YIN, J. and GENG, Z. (2010). Discover local causal network around a target to a given depth. *JMLR: Workshop and Conference Proceedings* **6** 191–202.

DEPARTMENT OF STATISTICS AND PROBABILITY, PEKING UNIVERSITY, BEIJING 100871, PR CHINA  
DEPARTMENT OF BIostatISTICS, UNIVERSITY OF PENNSYLVANIA SCHOOL OF MEDICINE,  
PHILADELPHIA, PA 19104, USA